Avicenna Journal of Phytomedicine (AJP)

Original Research Article

Synthesis of a niosome-based drug delivery system containing *Sambucus ebulus* extract: evaluation of its pro-apoptotic and anti-metastatic effects on HeLa cervical cancer cells

Marjan Bakhtiari[1], Mahsa Kavousi[1,*], Elahe Aliasgari[1]

[1] *Department of Biology, ET.C., Islamic Azad University, Tehran, Iran*

Article history:
Received: Jul 30, 2025
Received in revised form: Oct 06, 2025
Accepted: Oct 16, 2025
Epub ahead of print

**** Corresponding Author:***
Tel: +(98-21) 88830831
Fax: +(98-21) 88830831
ma.kavousi@iau.ac.ir

Keywords:
Targeted delivery
Surfactant vesicles
Cancer cell migration
Gene expression
Natural anticancer agents

Abstract

Objective: Cervical cancer affects over half a million women annually. Given the increasing interest in natural compounds as therapeutic agents, this study investigates the apoptotic and anti-metastatic effects of *Sambucus ebulus* extract—a medicinal plant with antioxidant and cytotoxic properties—encapsulated in niosomes on HeLa cervical cancer cells. Encapsulation in niosomes enhances the stability and cellular delivery of the extract, potentially improving its therapeutic efficacy.

Materials and Methods: Ethanolic extract of *S. ebulus* was prepared using Soxhlet extraction, followed by niosome synthesis and encapsulation of the extract. The physicochemical characterization of niosomes was performed using FTIR, DLS, and SEM analysis. Cytotoxicity of free niosomes, free extract, and loaded niosomes was assessed via MTT assay at 24, 48, and 72 hr. Cell cycle was analyzed using flow cytometry, while changes in *CASP8*, *CASP3*, *MMP2 and MMP9* gene expression were evaluated through real-time PCR.

Results: The mean size of synthesized niosomes was 366 nm. The MTT assay revealed that *S. ebulus* extract-loaded niosomes exerted the highest cytotoxic effect on HeLa cells, whereas no significant cytotoxicity was observed in the HOSEpiC normal cell line. Real-Time PCR showed a significant upregulation of apoptotic genes (*CASP3*, $p<0.001$; *CASP8*, $p<0.01$) and a downregulation of metastatic genes (*MMP2*, *MMP9*, $p<0.01$). Flow cytometry indicated that treatment with *S. ebulus* extract-loaded niosomes induced 50.09% total apoptosis ($p<0.01$), the highest among the tested groups. Cell cycle analysis demonstrated G0/G1 phase arrest at 24 hr treatment. Scratch assay confirmed a significant inhibition of cancer cell migration.

Conclusion: Encapsulation of *S. ebulus* within niosomes enhances the targeted delivery and efficacy of *S. ebulus* extract. Its apoptotic and anti-metastatic effects suggest potential for investigation as a novel therapeutic approach against cervical cancer.

Please cite this paper as:
Bakhtiari M, Kavousi M, Aliasgari E. Synthesis of a niosome-based drug delivery system containing *Sambucus ebulus* extract: evaluation of its pro-apoptotic and anti-metastatic effects on HeLa cervical cancer cells. Avicenna J Phytomed, 2025. Epub ahead of print.

Introduction

Cervical cancer remains a major global health burden, with over 500,000 new cases and high mortality annually (Arbyn et al. 2020). Limitations of chemotherapy and radiotherapy, including toxicity and drug resistance, underscore the need for alternative strategies (Zafar et al. 2025). Plant-derived bioactive compounds have emerged as promising agents with pro-apoptotic and anti-metastatic properties (Chaudhry et al. 2022).

Oxidative stress drives cancer progression via DNA damage, chronic inflammation, and metastasis (Solouki et al. 2021). Antioxidants from medicinal plants mitigate these effects by reducing oxidative injury, modulating oncogenic pathways, and enhancing cellular defenses (Kavousi and Delfani 2023). *Sambucus ebulus*, rich in flavonoids and phenolics, exhibits cytotoxic and anti-metastatic activities, though poor bioavailability and rapid metabolism hinder its clinical use (Bojar Doulaby et al. 2023).

Plant-derived antioxidants, including quercetin, curcumin, and resveratrol, inhibit tumor growth and induce apoptosis through PI3K/AKT, MAPK, and NF-κB pathway modulation (Ebadi et al. 2025; Ding and Yu 2025; Ouyang et al. 2014). Curcumin, notably, synergizes with chemotherapeutics, reducing resistance and improving outcomes in cervical and other cancers (Cacciola et al. 2023).

Nanotechnology enhances phytochemical therapy by improving delivery efficiency, stability, pharmacokinetics, and targeting (Minaei et al. 2025). Niosomes, a versatile class of non-ionic surfactant vesicles, offer superior stability, encapsulation of hydrophilic and lipophilic drugs, prolonged circulation, reduced leakage, and scalability compared with liposomes (Saadh et al. 2024). Formulations such as EGCG (Epigallocatechin gallate) and resveratrol in niosomes demonstrate enhanced uptake and anticancer efficacy (Li et al. 2022).

Niosomes efficiently improve the delivery of antioxidant-rich extracts, enhancing therapeutic outcomes while reducing toxicity (Minaei et al. 2025). In line with this strategy, Zargarani et al. (2025) demonstrated enhanced anticancer and antimetastatic effects of solanine-loaded nanoparticles in MCF-7 cells (Zargarani et al. 2025). This study investigates these effects in HeLa cells using cytotoxicity assays, gene expression profiling, and cell cycle analysis to assess the therapeutic potential of this nanoformulated extract.

Materials and Methods

Extraction of *S. ebulus* leaf extract

S. ebulus leaves were obtained from the National Gene Bank of Iran. After air-drying in a dark, moisture-free environment, 20 g of powdered leaves was mixed with 100 ml of 70% ethanol and subjected to Soxhlet extraction for 12 hr. The resulting extract was filtered, concentrated using a rotary evaporator, and reconstituted in double-distilled water to achieve a final concentration of 1500 µg/ml. The prepared extract was stored at 4°C until further analysis.

Preparation and characterization of Niosomes

Niosome nanoparticles (NPs) were prepared using the thin-film hydration method. Tween 80 (2 ml), Span 80 (1 ml; Merck, Germany), and cholesterol (1 mg) were dissolved in 20 ml of a chloroform: methanol mixture (2:1 v/v) to achieve the desired lipid composition, corresponding to a molar ratio of Tween 80:Span 80:Cholesterol of approximately 1:1.5:0.002 and a total lipid concentration of 159 mg/ml. Cholesterol comprised approximately 0.03% of the total lipid content.

The mixture was evaporated under reduced pressure using a rotary evaporator (Heidolph, Germany) at 60°C and 150 rpm for 30 min to form a thin lipid film. Hydration was performed with a hydro-alcoholic solution prepared by dissolving 40 mg of *S. ebulus* dried extract in 1–2 ml ethanol and adding it dropwise to 10 ml of

phosphate-buffered saline (PBS; pH 7.4) under stirring, resulting in a final extract concentration of 40 mg/100 ml. The lipid film was hydrated at 60°C for 30 min under rotation.

The hydrated suspension was sonicated for 15 min (Model 150 UPS, Iranian Technology Company Research Nasir, Iran) to reduce particle size. The resulting niosomes were stored at 4°C until further use. Characterization was performed using dynamic light scattering (DLS) for size distribution, X-ray diffraction (XRD) for crystallinity, scanning electron microscopy (SEM) for morphology, and Fourier-transform infrared spectroscopy (FTIR) for functional group analysis.

Evaluation of morphology and polydispersity index

The surface morphology of the *S. ebulus* extract-loaded niosomes was observed using a scanning electron microscope (SEM, Hitachi Model 3400N, Japan). Here, 15 µl sample of the niosomal suspension was placed on a glass slide and air dried at ambient temperature. Before scanning the samples in the SEM, they were fixed on a die and coated with a layer of gold to exclude charging effects. The SEM was operated with an accelerating voltage of 20 KV. The *S. ebulus* extract-loaded niosomes were diluted with distilled water at a ratio of 1:100. The droplet size and polydispersity index were measured using the Zeta Sizer instrument (Malvern Instruments, U.K). The measurements were performed at a light scattering angle of 90 degrees. Standard deviation against particle size and Zeta potential by Zetasizer was Zeta: 33.9±0.0002 and SEM: 4.438±500 nm.

Fourier transform infrared spectrum (FTIR)

FTIR (ALPHA II, Bruker, Germany) was performed to determine the interaction between drug and excipient and to investigate possible interactions between the substances used in the formulation. FTIR was used to measure the absorption peaks of both free niosomes and *S. ebulus* extract-loaded niosomes. The samples were prepared as KBr disks with a ratio of 2 mg *S. ebulus* extract-loaded niosomes to 200 mg KBr. The preparation was carried out using a hydrostatic press with a force of 275790.292 Pa for 5 min. The resulting spectra were obtained over the entire wavelength range from 4000 to 400 cm^{-1}.

Cell culture

HeLa cervical cancer cells were obtained from the Pasteur Institute Cell Bank (Iran) and cultured in RPMI 1640 medium, with HOSEpiC epithelial cells serving as the normal control. The cells were washed with PBS, treated with trypsin to facilitate detachment, and centrifuged at 1500 rpm for 7 min at 4°C. The resulting pellet was resuspended in complete RPMI 1640 medium supplemented with FBS and antibiotics, then transferred to a 75-ml flask and incubated at 37°C with 5% CO_2 and 95% relative humidity to ensure optimal cell viability and proliferation.

Cytotoxicity assessment

The cytotoxic effects of synthesized niosome nanoparticles were evaluated using the MTT assay. HeLa cervical cancer cells were seeded in 96-well plates at a density of 1×10^4 cells/well in RPMI 1640 medium supplemented with 10% fetal bovine serum (FBS) and incubated at 37°C in a humidified atmosphere containing 5% CO_2 for 24 hr to allow cell attachment. Cells were then treated with a range of concentrations (0.468–60 µg/ml) of free niosomes, free *S. ebulus* extract, and extract-loaded niosomes.

Following incubation for 24, 48, and 72 hr, 20 µl of MTT solution (5 mg/ml in PBS) was added to each well and incubated for an additional 4 hr under standard culture conditions. Formazan crystals formed by viable cells were dissolved in 150 µl dimethyl sulfoxide (DMSO), and absorbance was measured at 570 nm using an ELISA microplate reader (ChroMate,

The Netherlands). Relative cell viability (%) was calculated by comparing the absorbance of treated wells with that of the untreated control group. All experiments were performed in triplicate.

Due to technical limitations, representative well images could not be captured. Nonetheless, quantitative data from the MTT assay are comprehensively presented as dose–response curves in the Results section to clearly demonstrate cytotoxic effects while ensuring methodological transparency and scientific rigor.

Real- time PCR

To investigate the effects of niosome-encapsulated *S. ebulus* extract on apoptotic and metastatic pathways, total RNA was extracted from HeLa cells treated with the 72-hr IC_{50} dose using the RNX-Plus kit, following standard protocols. cDNA synthesis was performed with the Easy™ cDNA Synthesis Kit to ensure high-fidelity reverse transcription. Gene expression analysis was carried out using SYBR Green qPCR Master Mix to quantify transcript levels of apoptotic (*CASP3* and *CASP8*) and metastatic (*MMP2* and *MMP9*) markers, with *GAPDH* as the housekeeping gene.

Primers were designed by retrieving target gene sequences from NCBI and selecting exon-spanning regions using Primer3Plus. Primer properties were validated using OligoAnalyzer, and specificity was confirmed with NCBI Primer-BLAST. Synthesized primers were purchased from Metabion (Germany) and delivered in lyophilized form. Primer sequences used in this study are listed in Table 1.

The annealing temperatures for each primer pair were determined based on their calculated melting temperature (Tm), obtained using Primer-BLAST (NCBI) and OligoAnalyzer (IDT). Gradient PCR was then performed to empirically optimize the annealing conditions, and final temperatures were set at approximately 3–5°C below the predicted Tm, where specific and consistent amplification was observed.

Table 1. Primers list

Gene	Sequence	Tm (°C)	Product size (bp)
CASP3	F: 5′- TTTTTCAGAGGGGATCGTTG-3′ R: 5′- CGGCCTCCACTGGTATTTTA-3′	60 60	151
CASP8	F: 5′- TATGGCACTGATGGACAGGA-3′ R: 5′- GCAGAAAGTCAGCCTCATCC-3′	60.1 60	232
MMP2	F: 5′-AGTGGATGATGCCTTTGCTC-3′ R: 5′-GAGTCCGTCCTTACCGTCAA-3′	60.2 60.1	154
MMP9	F: 5′-TTGACAGCGACAAGAAGTGG-3′ R: 5′- TCACGTCGTCCTTATGCAAG- 3′	60 59.9	174
GAPDH	F: 5′- CGAGATCCCTCCAAAATCAA -3′ R: 5′- TTCACACCCATGACGAACAT-3′	60 59.8	170

Apoptosis assessment via flow cytometry

To evaluate apoptosis induced by niosome-encapsulated *S. ebulus* extract, HeLa cells were seeded in 24-well plates at a density of 1×10^5 cells/well and incubated for 24, 48, and 72 hr. Cells were treated with the corresponding IC_{50} concentrations determined for each time point. After treatment, cells were harvested by gentle trypsinization, washed twice with cold PBS, and centrifuged at 1500 rpm for 5 min. The pellet was resuspended in 100 µl of 1X binding buffer and stained with 5 µl Annexin V-FITC and 5 µl propidium iodide (PI) (Annexin V-FITC Apoptosis Detection Kit, BD Biosciences) for 15 min at room temperature in the dark.

Samples were immediately analyzed using a BD FACSCalibur flow cytometer equipped with 488 nm excitation and 530/575 nm emission filters. Compensation controls were applied to correct spectral overlap between FITC and PI. Forward scatter (FSC) and side scatter (SSC) were used to exclude debris, and doublets were discriminated using FSC-A/FSC-H gating.

Data were collected for at least 10,000 events per sample and analyzed with FlowJo software (version X).

The percentages of viable, early apoptotic, late apoptotic, and necrotic cells were quantified. Each experiment was performed in triplicate, and representative dot plots as well as plate images before cell harvesting are provided in the supplementary material for clarity.

Cell migration assay

To assess the anti-metastatic effects of the synthesized niosomes, HeLa cells were subjected to a wound healing assay following 72-hr IC_{50} treatment. Cells were seeded into gelatin-coated 6-well plates at a density of 10^5 cells per well, reaching 80% confluency before a uniform scratch was created using a pipette tip. Treated groups received IC_{50} concentrations of free extract, free niosomes, and extract-loaded niosomes. After 24 hr, migration was qualitatively assessed via microscopy by comparing scratch closure between control and treated groups.

Data analysis

Quantitative analysis was performed using GraphPad Prism 5, applying one-way ANOVA followed by the Tukey-Kramer post hoc test at a 95% confidence level to determine statistically significant differences.

Results

Characterization of the synthesized niosomes

FTIR analysis of *S. ebulus* extract-loaded niosomes

Fourier-transform infrared spectroscopy (FTIR) was utilized to characterize both free niosomes and *S. ebulus*-loaded niosomes, ensuring successful incorporation of the extract into the carrier system. Spectral data were analyzed using IRPal v.2.0 software.

For plain niosomes, characteristic peaks were observed at 3548 cm^{-1} (O-H stretching), 2923 cm^{-1} (CH_2 group), 1637 cm^{-1} (C=C stretching), 1617 cm^{-1} (NH_2 group), 1384 cm^{-1} (CH_3 group), 1093 cm^{-1} (C-N stretching), 895 cm^{-1} (=CH group), and 618 cm^{-1} (C-H bond).

In contrast, niosomes loaded with *S. ebulus* extract exhibited similar peaks with minor shifts, alongside two additional peaks at 3013 cm^{-1} (O-H dimer formation) and 475 cm^{-1} (C-Br bond). The appearance of these new peaks indicates interactions between the extract and the niosomal components, confirming successful loading and potential structural modifications that may influence biological activity (Figure 1).

DLS analysis of *S. ebulus* extract-loaded niosomes

The zeta potential spectrum, presented in Figure 2-A, illustrates the electrokinetic stability of the synthesized niosome. The measured zeta potential for *S. ebulus* extract-loaded niosomes was 39.1 mV, indicating a strong colloidal stability. This value suggests that the formulated niosome exhibits adequate repulsion between particles, minimizing aggregation and enhancing its structural integrity for potential biomedical applications. Also, Dynamic Light Scattering was utilized to determine the particle size of the synthesized niosome. As illustrated in Figure 2-B, the average particle size of extract-loaded niosomes was measured at 366 nm, reflecting a well-dispersed and stable nanoscale formulation, which is crucial for biomedical applications.

A

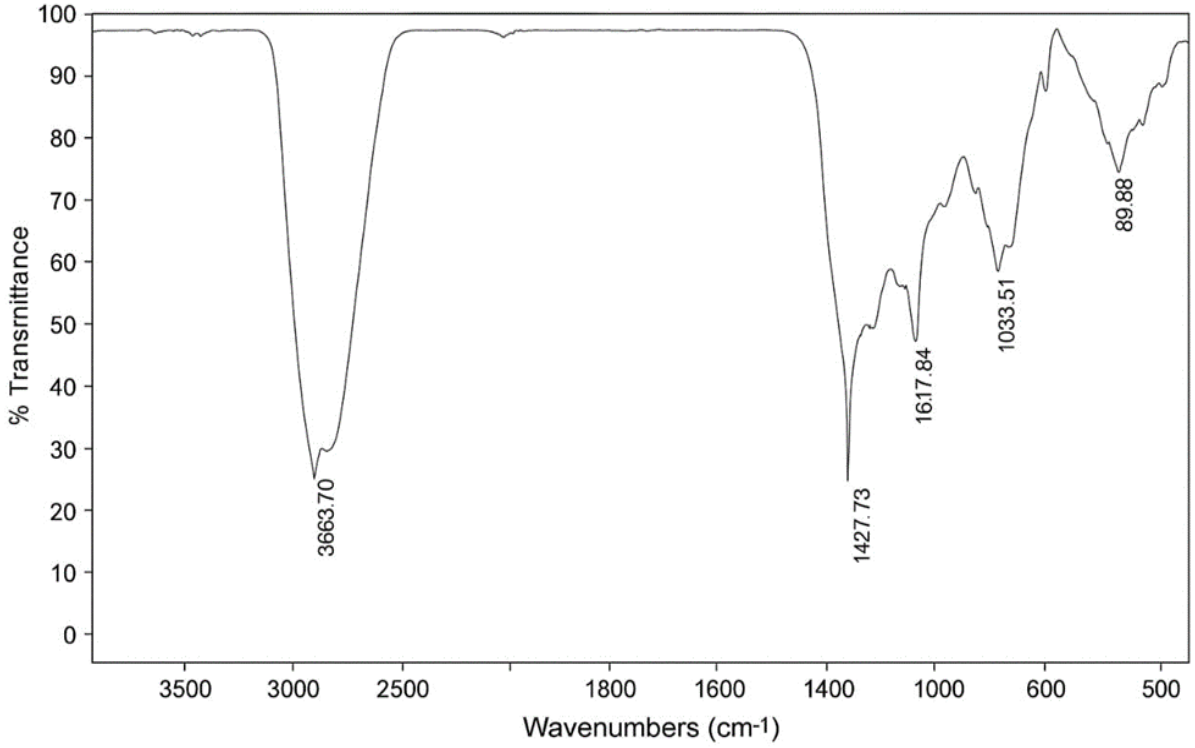

B

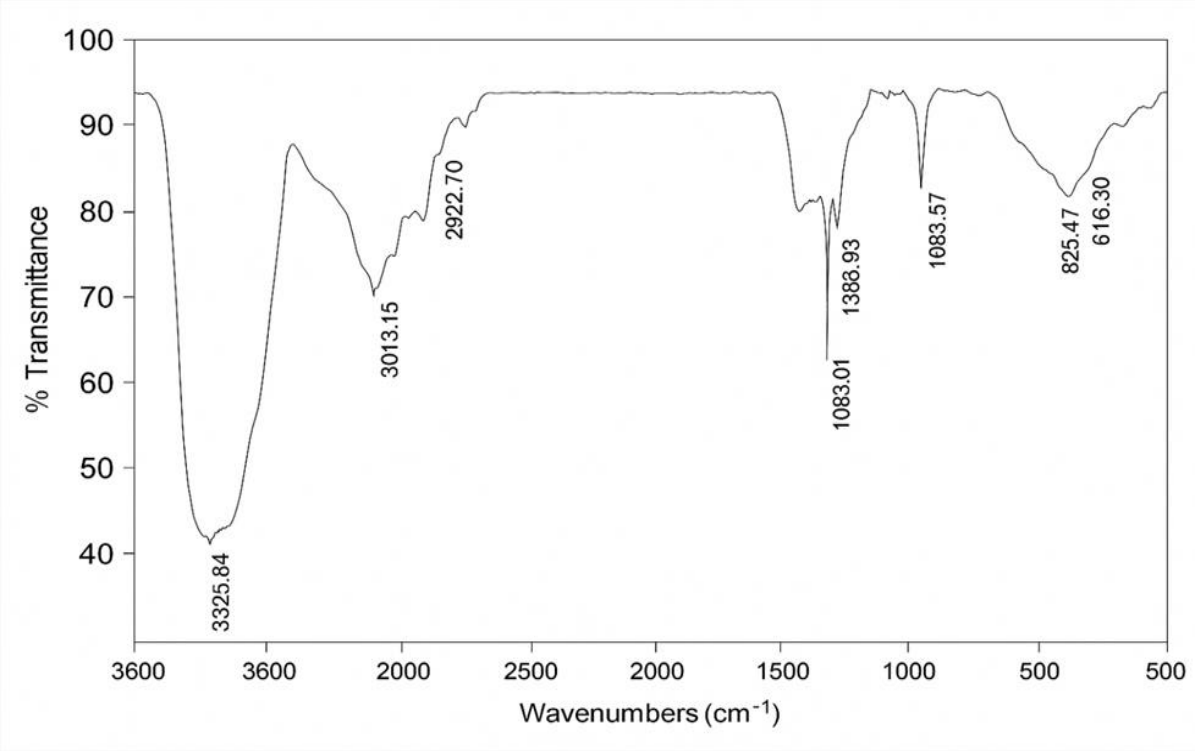

Figure 1. FTIR spectra for A) free niosomes and B) *S. ebulus* extract-loaded niosomes

A

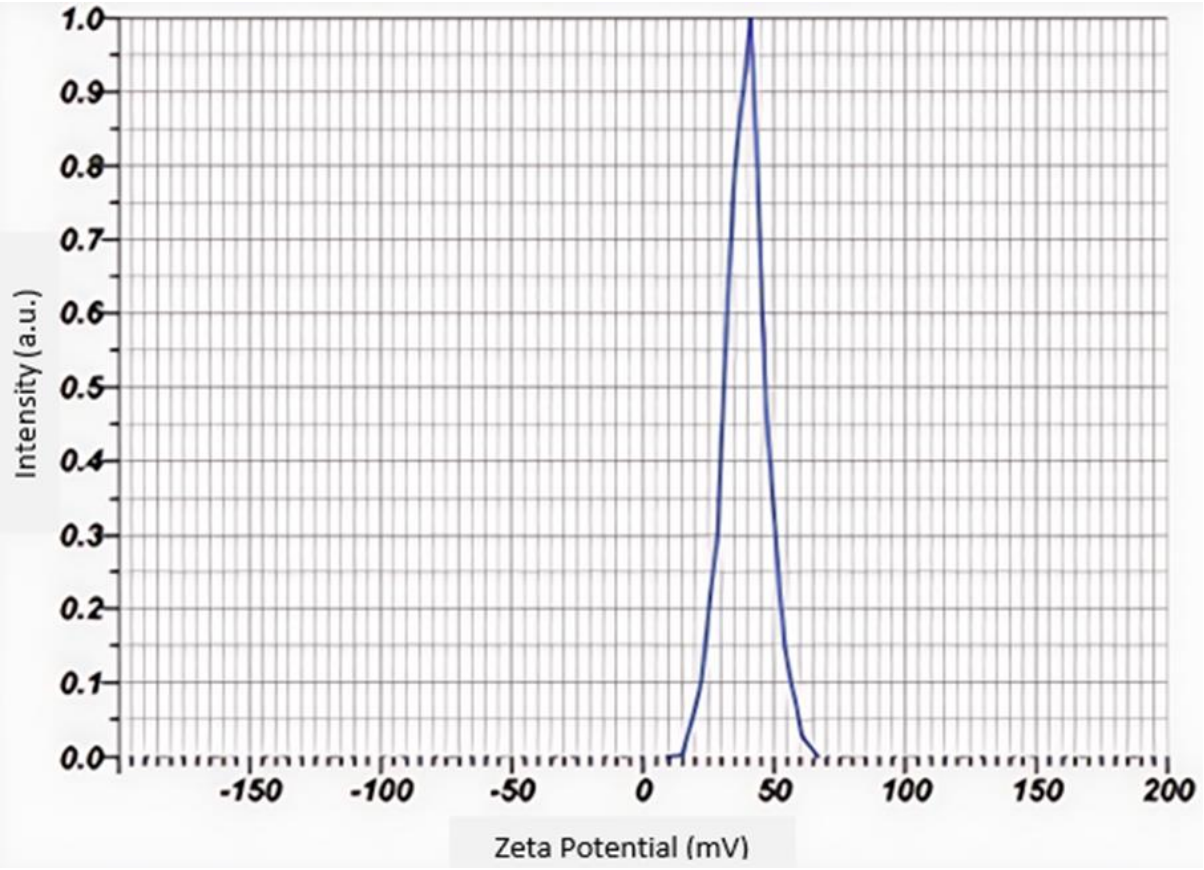

B

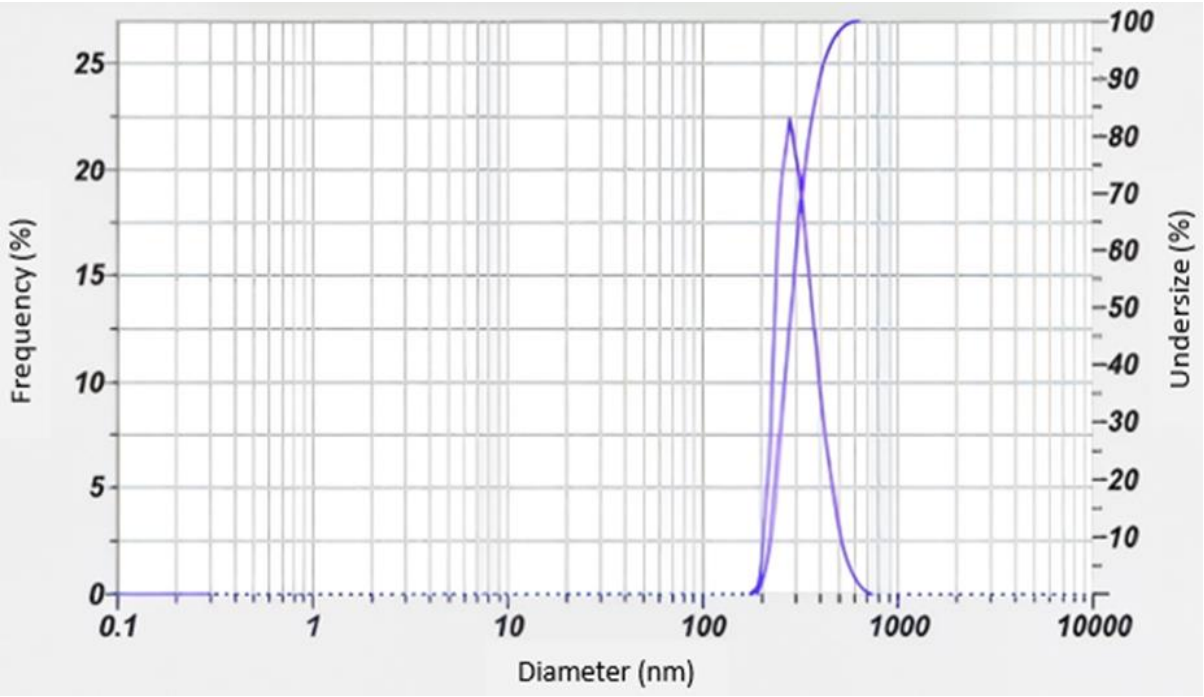

Figure 2. A) The spectrum obtained from the zeta potential with a value of 1.39 mV and B) Particle size of 366.5 nm for *S. ebulus* extract-loaded niosomes.

SEM analysis of *S. ebulus* extract-loaded niosomes

The morphological characteristics of the synthesized niosomes were examined using electron microscopy, with the results presented in Figure 3. As observed, the niosomes exhibit a homogeneous and polygonal structure, indicating a well-defined and stable formulation. This structural uniformity suggests controlled synthesis parameters, which contribute to the overall stability and potential functionality of the niosomes in biomedical applications.

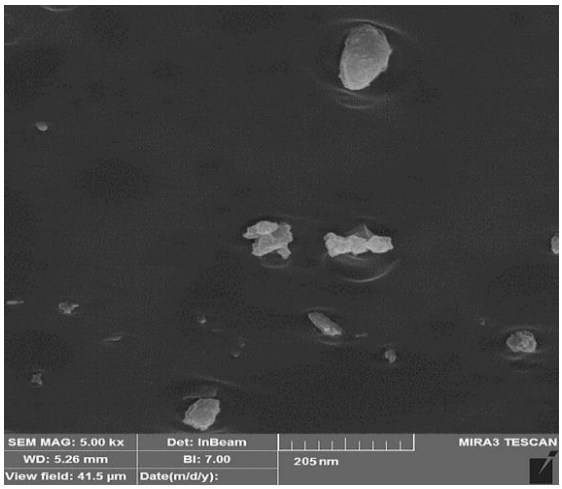

Figure 3. Morphological characterization of optimized *S. ebulus* extract-loaded niosomes using scanning electron microscope.

Cell viability assessment of HeLa and HOSEpiC normal cells

The results demonstrated a time-dependent decrease in HeLa cell viability, with increasing cytotoxic effects observed over 24, 48, and 72 hr (Figure 4; Tables S2–S4). The IC_{50} values progressively declined, indicating enhanced extract potency over time (Table S1). Notably, the *S. ebulus* extract-loaded niosome group exhibited significantly greater cytotoxicity against cancer cells compared to the free extract ($p < 0.05$) and free niosomes ($p < 0.001$), particularly at 72 hr. This effect is likely attributed to the acidic microenvironment of cancer cells, which enhances niosome dissolution and targeted delivery. In contrast, normal cells showed higher viability in the *S. ebulus* extract-loaded niosome group than in the free *S. ebulus* extract group, confirming the selective cytotoxicity of the encapsulated extract against HeLa cells while sparing healthy cells (Figure 4; Tables S5–S7). These findings highlight the potential therapeutic advantage of niosomal encapsulation in optimizing *S. ebulus* extract efficacy for cancer treatment.

Gene expression analysis

CASP3 expression exhibited a time-dependent increase in both treatment groups compared to the control. In the free *S. ebulus* extract-treated group, *CASP3* expression was elevated by 1.10 fold at 24 hr ($p = 0.05$), 1.18 fold at 48 hr ($p = 0.05$), and 1.25 fold at 72 hr ($p = 0.05$). No significant change was observed in the free niosome group at any time point ($p > 0.05$, NS). In contrast, the *S. ebulus* extract-loaded niosome group showed significantly higher *CASP3* expression, with 1.40 fold at 24 hr ($p < 0.01$), 1.73 fold at 48 hr ($p < 0.01$), and 1.78 fold at 72 hr ($p < 0.01$) relative to control. These findings indicate that encapsulation of *S. ebulus* extract within niosomes markedly enhances *CASP3* expression over time, thereby potentiating apoptotic activity (Figure 5).

CASP8 expression showed a significant and time-dependent increase in both treatment groups compared to the control. In the free *S. ebulus* extract-treated group, *CASP8* expression increased by 1.20 fold at 24 hr ($p < 0.05$), 1.47 fold at 48 h ($p < 0.05$), and 1.58 fold at 72 hr ($p < 0.05$). In the free niosome group, no significant changes were observed at any time point ($p > 0.05$, NS). Conversely, the *S. ebulus* extract-loaded niosome group exhibited markedly higher *CASP8* expression, with 1.24 fold at 24 hr ($p < 0.01$), 1.46 fold at 48 h ($p < 0.01$), and 1.76 fold at 72 hr ($p < 0.01$) relative to control. These results suggest that encapsulation of *S. ebulus* extract within niosomes significantly enhances *CASP8* expression over time, indicating potentiation of apoptotic signaling pathways (Figure 5).

S. ebulus Niosomes induce apoptosis in HeLa cells

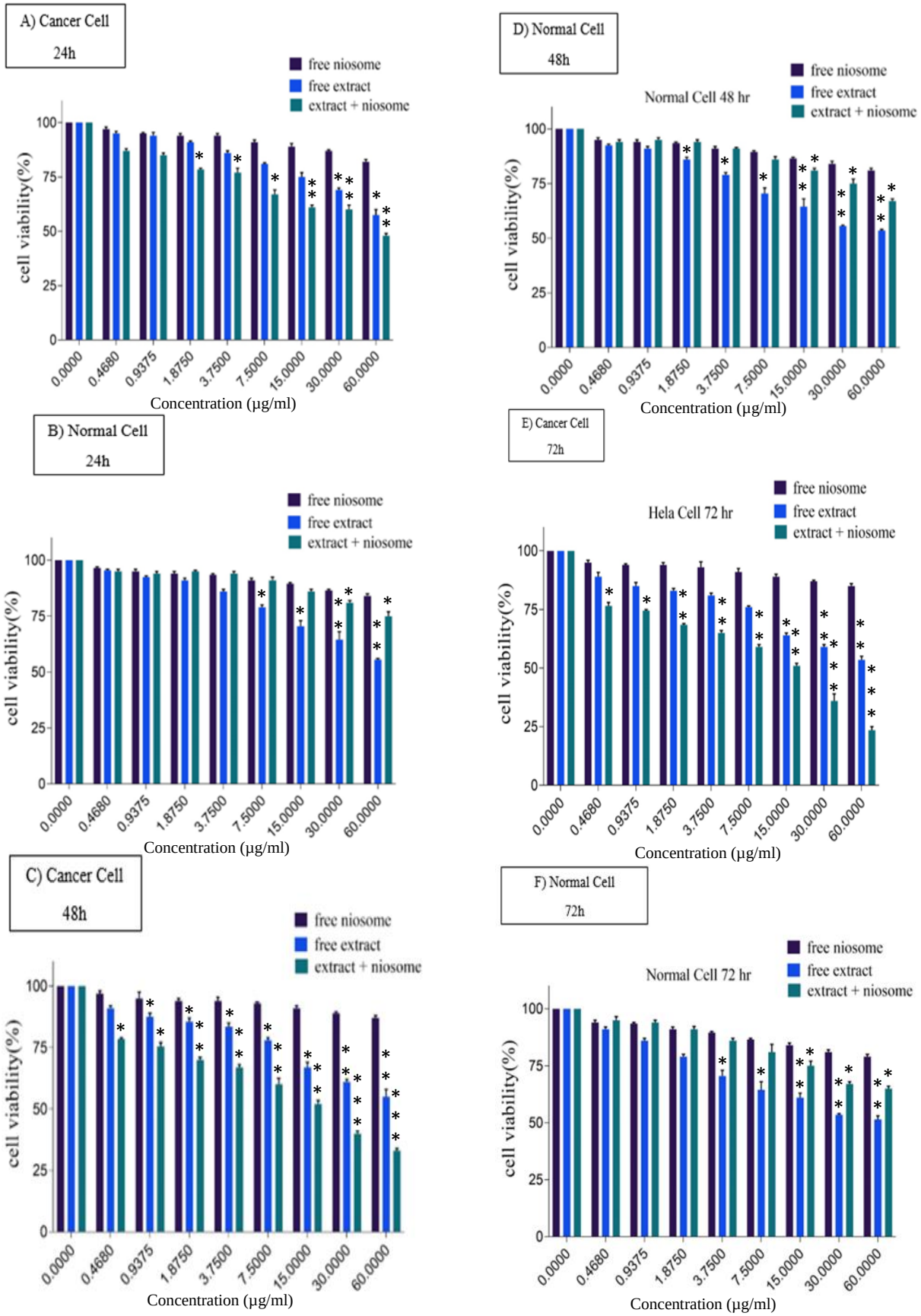

Figure 4. Survival of HeLa and HOSEpiC cells treated with free *S. ebulus extract*, free niosomes, and *S. ebulus* extract-loaded niosomes. (*p<0.05,**p<0.01, ***p<0.001; statistical analysis performed using one-way ANOVA followed by Tukey's test post hoc**)**

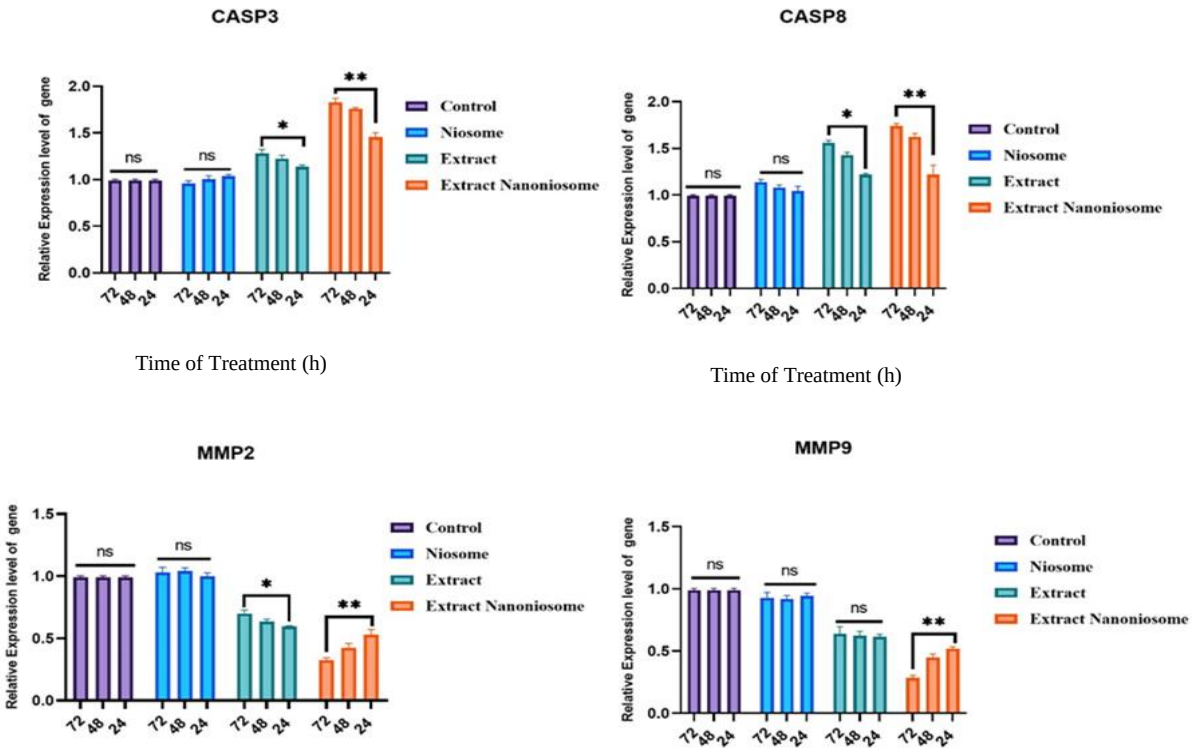

Figure 5. Gene expression results in the free *S. ebulus* extract and *S. ebulus* extract-loaded niosome treatment. (*p<0.05 and **p<0.01; statistical analysis performed using one-way ANOVA followed by Tukey's post hoc test)

MMP2 expression showed a significant and time-dependent decrease in both treatment groups compared to the control. In the free *S. ebulus* extract-treated group, *MMP2* expression decreased by 0.60 fold at 24 hr ($p<0.05$), 0.68 fold at 48 hr ($p<0.05$), and 0.72 fold at 72 hr ($p<0.05$). No significant change was observed in the free niosome group at any time point ($p>0.05$, NS). In contrast, the *S. ebulus* extract-loaded niosome group exhibited a markedly greater downregulation of *MMP2* expression, with 0.50 fold at 24 hr ($p<0.01$), 0.40 fold at 48 hr ($p<0.01$), and 0.32 fold at 72 hr ($p<0.01$) relative to control. These results suggest that encapsulation of *S. ebulus* extract within niosomes significantly enhances the inhibitory effect on *MMP2* expression over time, indicating a potent anti-metastatic potential (Figure 5).

MMP9 expression demonstrated differential regulation in the two treatment groups over time. In the free *S. ebulus* extract-treated group, *MMP9* expression exhibited a non-significant decrease, with fold changes of 0.57 at 24 hr ($p > 0.05$), 0.58 at 48 hr ($p>0.05$), and 0.60 at 72 hr ($p>0.05$), indicating no statistically significant modulation. In contrast, the *S. ebulus* extract-loaded niosome group showed a significant, time-dependent downregulation of *MMP9* expression. Specifically, *MMP9* expression decreased by 0.51 fold at 24 hr ($p<0.01$), 0.47 fold at 48 hr ($p<0.01$), and 0.28 fold at 72 hr ($p<0.01$) compared to the control. These findings suggest that encapsulation of *S. ebulus* extract within niosomes markedly enhances the inhibitory effect on *MMP9* expression, highlighting its potential role in suppressing metastatic activity.

Flow cytometry analysis

Flow cytometry analysis using Annexin V-FITC/PI staining demonstrated a significant increase in total apoptosis (early and late stages) in HeLa cells treated with niosome-encapsulated *S. ebulus* extract compared to those treated with free extract or free niosomes ($p < 0.01$). The dot plots were divided into four quadrants, each representing a distinct cell population: Q_1

(Annexin V^-/PI^+ – necrotic cells), Q_2 (Annexin V^+/PI^+ – late apoptotic cells), Q_3 (Annexin V^+/PI^- – early apoptotic cells), and Q_4 (Annexin V^-/PI^- – viable cells). In the extract-loaded niosome group, a marked elevation was observed in both Q_2 and Q_3 quadrants, indicating enhanced apoptotic induction. Notably, the proportion of early apoptotic cells (Q_3) was significantly higher at 72 hr, suggesting that the nanoformulation initiates apoptosis effectively before progression to late stages. In contrast, the free extract and free niosome groups showed minimal changes in apoptotic quadrants and retained high percentages in Q_4, reflecting limited cytotoxicity. These results highlight the superior efficacy of niosomal encapsulation in promoting apoptosis, likely due to improved cellular uptake and sustained release of bioactive compounds. The reduction in viable cells (Q_4) and concurrent increase in apoptotic populations (Q_2 and Q_3) underscore the potential of this nanoformulation as a targeted therapeutic strategy against cervical cancer (Figures 6 and 7).

HeLa cells invasion analysis

The scratch assay revealed significant differences in cell migration among the experimental groups. The control and free niosome groups exhibited the highest migration ability, indicating minimal inhibitory effects. In contrast, the free extract-treated group displayed a moderate reduction in migration compared to the control and free niosome groups, suggesting partial suppression of cellular motility (Figure 8).

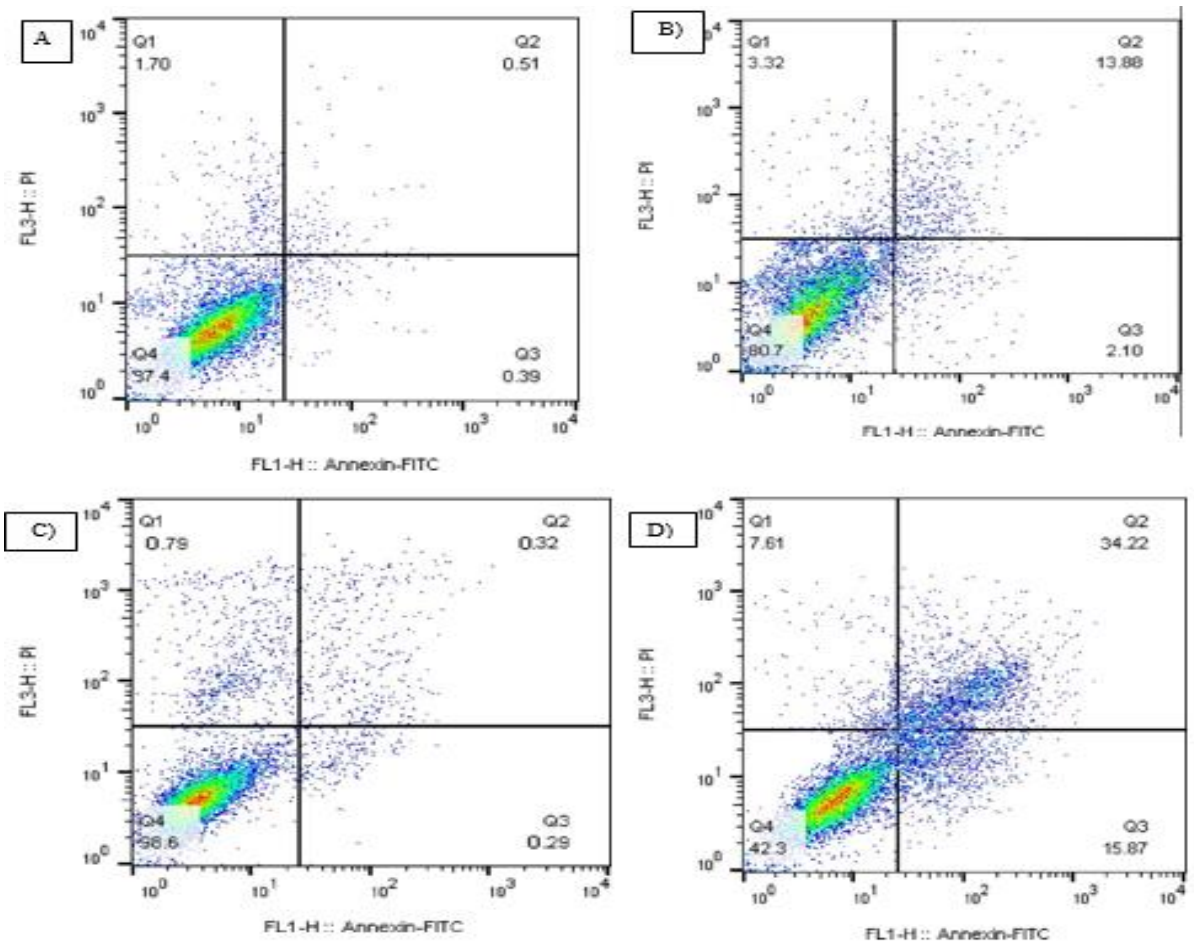

Figure 6. Flowcytometry analysis of HeLa Cells in A) non- treated, B) free *S. ebulus* extract, C) free niosome and D) *S. ebulus* extract-loaded niosomes.

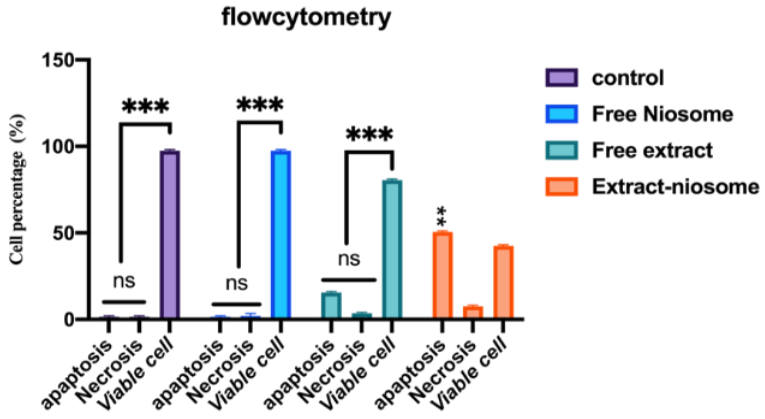

Figure 7. Comparison of cell death induction in the studied cells treated with free niosomes, free *S. ebulus* extract and *S. ebulus* extract-loaded niosomes (**p<0.01 and ***p<0.001; statistical analysis performed using one-way ANOVA followed by Tukey's post hoc test)

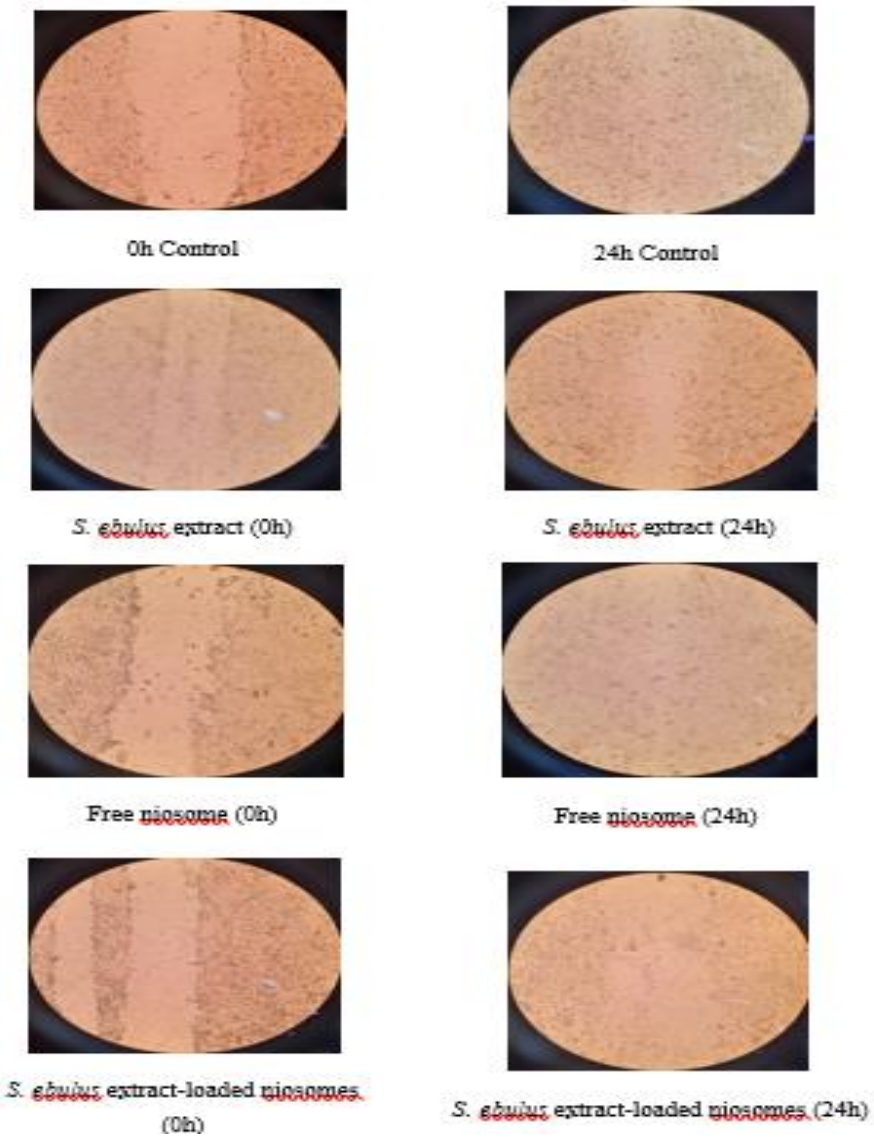

Figure 8. Scratch test for free *S. ebulus* extract, free niosome and *S. ebulus* extract-loaded niosomes 0 and 24 hr after treatment.

Discussion

The encapsulation of *S. ebulus* extract within niosomes represents a sophisticated approach in cancer therapy, merging nanotechnology with bioactive compounds to enhance therapeutic efficacy (Saadh et al. 2024; Manzari-Tavakoli et al. 2024; Mestre 2021). This study underscores the ability of extract-loaded niosomes to induce apoptosis and suppress metastasis more effectively than both free extract and free niosomes, highlighting the synergy between natural compounds and advanced drug delivery systems.

One of the greatest challenges in cancer treatment is the lack of specificity of conventional therapeutics, which often indiscriminately damage both healthy and malignant cells (Kaur et al. 2023). Niosomal encapsulation offers several advantages that directly address these limitations (Yasamineh et al. 2022). The structure of niosomes provides enhanced protection for bioactive molecules, preventing premature degradation while facilitating targeted intracellular release (Yasamineh et al. 2022). This controlled delivery mechanism not only increases drug efficacy but also improves patient outcomes by minimizing toxic side effects (Odiba et al. 2016).

The choice of a plant-derived therapeutic agent further strengthens this approach. Natural compounds possess intrinsic multifunctional properties, modulating multiple oncogenic pathways simultaneously, unlike synthetic agents that typically have a singular mode of action (Dehelean et al. 2021; Yang et al. 2025). *S. ebulus* extract is known for its rich composition of polyphenols, flavonoids, and alkaloids, which collectively exhibit anti-proliferative, pro-apoptotic, and anti-metastatic effects (Cvetanović 2020). However, its full potential is often limited by poor bioavailability. Niosomal encapsulation circumvents this issue by stabilizing the extract and ensuring sustained cellular uptake, thereby maximizing its therapeutic benefits (Saadh et al. 2024).

Cancer cells evade apoptosis, allowing uncontrolled proliferation and survival (Wang et al. 2013). This study demonstrates significant activation of apoptotic pathways upon treatment with extract-loaded niosomes. *CASP3* expression was markedly upregulated (1.75 fold, $p<0.001$), confirming the involvement of execution-phase apoptosis. Similarly, *CASP8*, a crucial initiator of extrinsic apoptosis, showed a 1.76 fold increase ($p<0.01$), reinforcing the role of the extract-loaded niosomes in promoting cell death. Flow cytometry analysis revealed a notable increase in total apoptosis (50.09%, $p<0.01$), surpassing the effects observed in free extract and free niosomes. The ability to induce cell cycle arrest at G0/G1 phase further supports the therapeutic impact of the encapsulated extract, disrupting the cell cycle and reducing cancer cell replication rates.

Beyond apoptosis, cancer metastasis remains a critical challenge, leading to aggressive tumor progression and poor prognosis (Guan 2015). The findings of this study highlight the strong anti-metastatic effects of *S. ebulus* extract when delivered through niosomes. *MMP2* and *MMP9*, key matrix metalloproteinases responsible for extracellular matrix degradation and tumor invasion, were significantly suppressed. *MMP2* expression decreased 0.32 fold, while *MMP9* levels dropped 0.28 fold, effectively limiting invasive behavior. The scratch assay further confirmed that extract-loaded niosomes drastically reduced cell migration, reinforcing their therapeutic potential in preventing tumor dissemination.

A crucial distinction between traditional chemotherapeutics and niosomal systems is their impact on normal cells (Kratz and Warnecke 2012). Many existing treatments exert significant cytotoxicity on healthy tissues, leading to debilitating side effects (Corrie 2008). The data from this study demonstrate that niosome-

encapsulated *S. ebulus* extract exhibits selective cytotoxicity, targeting HeLa cells while sparing normal HOSEpiC cells. This effect is likely attributed to the pH-responsive behavior of niosomes, which preferentially dissolve in the acidic microenvironment of cancer cells, ensuring localized drug delivery and reducing systemic toxicity. This selectivity is paramount in improving patient quality of life and overcoming the major challenge of chemotherapy-associated side effects (Mao et al. 2024).

The implications of these findings suggest that *S. ebulus*-loaded niosomes not only induce apoptosis but actively prevent metastasis, marking a significant advancement in nanotechnology-based cancer treatment. Their dual-action mechanism, combined with high selectivity for cancer cells, underscores the therapeutic potential of bioengineered nanocarriers in precision oncology. Further studies, including *in vivo* and clinical trials, are essential to validate their efficacy, refine their formulation, and establish standardized dosing strategies for future applications in personalized cancer therapy.

Acknowledgment

Authors have especial thanks for Research Laboratory for Tehran Branch of Islamic Aazad university laboratory staffs for their technical help.

Conflicts of interest

Authors declare that there is no conflict of interest.

Funding

The authors received no financial support for the research, authorship, and/or publication of this article.

Authors' Contributions

Mahsa Kavousi designed the study and supervised the work. Marjan Bakhtiari conducted the experiments, while Elahe Aliasgari analyzed the results. Marjan Bakhtiari drafted the manuscript, and Mahsa Kavousi contributed to revising it and approved the final version.

References

Arbyn M, Weiderpass E, Bruni L, de Sanjosé S, Saraiya M, Ferlay J, Bray F (2020) Estimates of incidence and mortality of cervical cancer in 2018: a worldwide analysis. Lancet Glob Health 8(2):E191-E203 doi:10.1016/S2214-109X(19)30482-6

Baranei M, Taheri RA, Tirgar M, et al. (2021) Anticancer effect of green tea extract (GTE)-loaded pH-responsive niosome coated with PEG against different cell lines. Mater Today Commun 26(9):101751 doi:10.1016/j.mtcomm.2020.101751

Bojar Doulaby F, Kavousi M, Jamshidian F (2023) Effect of Dioscorea extract on Bax and Bcl-2 gene expression in MCF-7 and HFF cell lines. Egypt J Med Hum Genet 24:70 doi:10.1186/s43042-023-00450-w

Cacciola NA, Cuciniello R, Petillo GD, Piccioni M, Filosa S, Crispi S (2023) An overview of the enhanced effects of curcumin and chemotherapeutic agents in combined cancer treatments. Int J Mol Sci 24(16):12587 doi:10.3390/ijms241612587

Chaudhry GES, Akim A Md, Sung YY, Sifzizul TMT (2022) Cancer and apoptosis: the apoptotic activity of plant and marine natural products and their potential as targeted cancer therapeutics. Front Pharmacol 13:842376 doi:10.3389/fphar.2022.842376

Corrie PG (2008) Cytotoxic chemotherapy: clinical aspects. Medicine 36:24–28 doi:10.1016/j.mpmed.2007.10.012

Cvetanović A (2020) Sambucus ebulus L., antioxidants and potential in disease pathology. In: Preedy VR (Ed) Pathology: Oxidative Stress and Dietary Antioxidants. Academic Press, Elsevier, London, 321–333. doi:10.1016/B978-0-12-815972-9.00031-7

Dehelean CA, Marcovici I, Soica C, Mioc M, Coricovac D, Iurciuc S, Cretu OM, Pinzaru I (2021) Plant-derived anticancer compounds as new perspectives in drug discovery and alternative therapy. Molecules 26(4):1109 doi:10.3390/molecules26041109

Ding Y, Yu Y (2025) Therapeutic potential of

flavonoids in gastrointestinal cancer: focus on signaling pathways and improvement strategies. Mol Med Rep 31(4):109 doi:10.3892/mmr.2025.13474

Ebadi M, Kavousi M, Farahmand M (2025) Investigation of the apoptotic and antimetastatic effects of nano-niosomes containing the plant extract Anabasis setifera on HeLa: in vitro cervical cancer study. Chem Biodivers 22:e202402599 doi:10.1002/cbdv.202402599

Guan X (2015) Cancer metastases: challenges and opportunities. Acta Pharm Sin B 5(5):402–418 doi:10.1016/j.apsb.2015.07.005

Homaeii S, Kavousi M, Ali Asgari E (2025) Investigating the apoptotic and antimetastatic effect of daphnetin-containing nano niosomes on MCF-7 cells. Adv Cancer Biol Metastasis 14:100139 doi:10.1016/j.adcanc.2025.100139

Kaur R, Bhardwaj A, Gupta S (2023) Cancer treatment therapies: traditional to modern approaches to combat cancers. Mol Biol Rep 50(11):9663–9676 doi:10.1007/s11033-023-08809-3

Kavousi M, Delfani A (2023) Solanum pseudo-capsicum effects on Bax and Bcl-2 gene expression and apoptosis in MCF-7 cell line. Genetika 55(2):523–536 doi:10.2298/GENSR2302523K

Kratz F, Warnecke A (2012) Finding the optimal balance: challenges of improving conventional cancer chemotherapy using suitable combinations with nano-sized drug delivery systems. J Control Release 164(2):221–235 doi:10.1016/j.jconrel.2012.05.045

Li D, Martini N, Wu Z, Chen S, Falconer JR, Locke M, Zhang Z, Wen J (2022) Niosomal nanocarriers for enhanced dermal delivery of epigallocatechin gallate for protection against oxidative stress of the skin. Pharmaceutics 14(4):726 doi:10.3390/pharmaceutics14040726

Manzari-Tavakoli A, Babajani A, Tavakoli MM, Safaeinejad F, Jafari A (2024) Integrating natural compounds and nanoparticle-based drug delivery systems: a novel strategy for enhanced efficacy and selectivity in cancer therapy. Cancer Med 13(5):e7010 doi:10.1002/cam4.7010

Mao X, Wu S, Huang D, Li C (2024) Complications and comorbidities associated with antineoplastic chemotherapy: rethinking drug design and delivery for anticancer therapy. Acta Pharm Sin B 14(7): 2901-2926 doi:10.1016/j.apsb.2024.03.006

Mestre HACB (2021) Development of ethosomes as skin carriers for *Sambucus nigra* L. extracts. MSc Thesis, Faculdade de Farmácia, Universidade de Lisboa, Lisbon, Portugal.

Minaei S, Kavousi M, Jamshidian F (2025) The apoptotic and anti-metastatic effects of niosome kaempferol in MCF-7 breast cancer cells. Sci Rep 15:20741 doi:10.1038/s41598-025-07221-0

Odiba A, Ukegbu C, Anunobi O, Chukwunonyelum I, Esemonu J (2016) Making drugs safer: improving drug delivery and reducing the side effect of drugs on the human biochemical system. Nanotechnol Rev 5(2):183–194 doi:10.1515/ntrev-2015-0055

Ouyang L, Luo Y, Tian M, Zhang SY, Lu R, Wang JH, Kasimu R, Li X (2014) Plant natural products: from traditional compounds to new emerging drugs in cancer therapy. Cell Prolif 47(6):506–515 doi:10.1111/cpr.12143

Saadh MJ, Mustafa MA, Kumar S, Gupta P, Pramanik A, Rizaev JA, Shareef HK, Alubiady MHS, Al-Abdeen SHZ, Shakier HG, Alaraj M, Alzubaidi LH (2024) Advancing therapeutic efficacy: nanovesicular delivery systems for medicinal plant-based therapeutics. Naunyn Schmiedebergs Arch Pharmacol 397(10):7229–7254 doi:10.1007/s00210-024-03104-9

Solouki N, Mohammadi-Gollou A, Sagha M, Mohammadzadeh-Vardin M (2021) Origanum vulgare extract induces apoptosis in Molt-4 leukemic cell line. J Cell Biotechnol 6(2):105–112 doi:10.3233/JCB-200026

Wang RA, Li QL, Li ZS, Zheng PJ, Zhang HZ, Huang XF, Chi SM, Yang AG, Cui R (2013) Apoptosis drives cancer cells proliferate and metastasize. J Cell Mol Med 17(1):205–211 doi:10.1111/j.1582-4934.2012.01663.x

Yang LY, Lei SZ, Xu WJ, Lai YX, Zhang YY, Wang Y, Wang Z (2025) Rising above: exploring the therapeutic potential of natural product-based compounds in human cancer treatment. Tradit Med Res 10(13):18 doi:10.53388/TMR20240618001

Yasamineh S, Yasamineh P, Ghafouri Kalajahi H, Gholizadeh O, Yekanipour Z, Afkhami

H, Eslami M, Kheirkhah AH, Taghizadeh M, Yazdani Y, Dadashpour M (2022) A state-of-the-art review on the recent advances of niosomes as a targeted drug delivery system. Int J Pharm 624:121878 doi: 10.1016/j.ijpharm.2022.121878

Zafar A, Khatoon S, Khan MJ, Abu J, Naeem A (2025) Advancements and limitations in traditional anti-cancer therapies: a comprehensive review of surgery, chemotherapy, radiation therapy, and hormonal therapy. Discov Oncol 16(1):607 doi:10.1007/s12672-025-02198-8

Zargarani N, Kavousi M, Aliasgari E (2025) A potential new strategy for BC treatment: NPs containing solanine and evaluation of its anticancer and antimetastatic properties. BMC Cancer 25(1):860 doi:10.1186/s12885-025-14249-y

Supplementary

Supplementary Table 1. Supplementary materials 1

IC_{50}(µg/ml) Tre/ Cell Line	Free extract	Extract + Niosomes
24/ Normal cells	81	30526
48/Normal cells	72	15260
72/Normal cells	60	7681
24/ HeLa cells	86	54
48/HeLa cells	73	22
72/HeLa cells	60	17

Supplementary Table 2. HeLa cells, 24 hr after treatment

Treatments Concentration(µg/ml)	Free Niosome	Free Extract	Extract + Niosome
60	82 ± 1	57.5 ± 2.5	48 ± 1
30	87 ± 0.53	69 ± 1	60 ±2
15	89 ± 1.41	75 ± 2	61 ± 1
7.5	91 ± 1	81 ± 1	67 ± 2
3.75	94 ± 1	86 ± 0.5	77 ± 2
1.875	94 ± 1	91 ± 1	78.5± 0.5
0.9375	95 ± 0.5	94 ±1.5	85 ± 1
0.468	97 ±1	95 ±1	87 ±1

Supplementary Table 3. HeLa cells. 48 hr after treatment

Treatments Concentration(µg/ml)	Free Niosomes	Free Extract	Eextract + Niosomes
60	87 ± 1	55 ± 3	33 ± 1
30	89 ± 0.5	61 ± 1	40 ± 1
15	91 ± 1	67 ± 2	52 ±1.52
7.5	93 ± 0.5	78 ±1	60 ±2.5
3.75	94 ± 1.5	83.5 ± 1.5	67 ± 1
1.875	94 ± 1	85.5 ±1.5	70 ± 1
0.9375	95± 2.5	87.5 ± 1.5	75.5 ± 1.5
0.468	97 ± 1	91 ± 1	78.5 ± 0.5

Supplementary Table 4. HeLa cells, 72 hr after treatment

Tratment Concentration (µg/ml)	Free Niosomes	Free Extract	Extract + Niosomes
60	85 ±1	53.5 ± 1.5	23.5 ±1.5
30	87 ± 0.5	59 ± 1	36 ± 3
15	89 ± 1	64 ±1	51 ± 1
7.5	91 ± 1.5	76 ± 0.5	59 ± 1
3.75	93 ± 2.3	81 ± 1	65 ± 1
1.875	94 ± 1	83 ± 1	68.5 ± 0.5
0.9375	94 ± 0.5	85 ± 1.5	74.5 ± 0.5
0.468	95 ± 1	89 ± 1.8	76.5 ±1.5

Supplementary Table 5. Normal cells, 24 hr after treatment

Treatments Concentration(µg/ml)	Free Niosomes	Free Extract	Extract + Niosomes
60	84 ± 1	55.5 ± 0.5	75 ± 2
30	86.5 ± 0.5	64.5±3.5	81 ± 1
15	89.5 ± 0.5	70.5 ± 2.5	86 ± 1
7.5	91 ± 1	79 ± 1	91 ± 1.45
3.75	93.5 ± 0.5	86 ± 1	94 ± 1
1.875	94 ± 1	91 ± 1	95 ± 0.5
0.9375	95 ± 1	92.5 ± 0.5	94 ± 1
0.468	96.5 ± 0.5	95.5 ± 0.5	95 ± 1

Supplementary Table 6. Normal cells, 48 hr after treatment

Treatments / Concentration (µg/ml)	Free Niosomes	Free Extract	Extract + Niosomes
60	81 ± 1	53.5 ± 0.5	67 ±1
30	84 ± 1.2	55.5 ± 0.5	75 ± 2
15	86.5 ± 0.5	64.5 ± 3.5	81 ± 1
7.5	89.5 ± 0.5	70.5 ± 2.5	86 ± 1.3
3.75	91 ±1	79 ± 1	91 ± 0.5
1.875	93.5 ± 0.5	86 ± 1	94 ± 1
0.9375	94 ± 1	91 ± 1	95 ± 1
0.468	95 ± 1	92.5 ± 0.5	94 ± 1

Supplementary Table 7. Normal cells, 72 hr after treatment

Treatments / Concentration(µg/ml)	Free Niosomes	Free Extract	Extract + Niosomes
60	79 ± 1	51.5 ± 1.5	65 ± 1
30	81 ±1	53.5 ± 0.5	67 ± 1
15	84 ±1	61 ± 2	75 ± 2
7.5	86.5 ± 0.5	64.5 ± 3.5	81 ± 3.39
3.75	89.5 ± 0.5	70.5 ± 2.5	86 ± 1
1.875	91 ± 1	79 ± 1	91 ± 1.23
0.9375	93.5 ± 0.5	86 ± 1	94 ± 1
0.468	94 ±1	91 ± 1	95 ±1.5